AAPG

An International Geological Organization

BULLETIN

VOLUME 84 • NUMBER 11 • NOVEMBER 2000 • ISSN 0149-1423

Evaluation of possible gas microseepage mechanisms

Alton Brown

ABSTRACT

Petroleum microseepage anomalies over petroleum accumulations are commonly explained by rapid, vertical migration of colloidal gas bubbles through fracture networks. This article is a theoretical analysis of this mechanism and of continuous gas-phase flow in fractures. The gas-bubble ascent mechanism is much slower than reported microseepage velocities, so it cannot account for observed microseepage. In contrast, continuous gas-phase flow through fractures can equal or exceed reported microseepage velocity, while maintaining total flux low enough so that petroleum accumulations can exist for geological lengths of time. Fracture entry pressure for bubbles is more than twice that of a continuous gas phase, so continuous gas-phase migration also requires a lower pressure threshold before initiating seepage. Vertical microseepage is therefore best explained by the same mechanism interpreted for macroseepage.

Although this article provides a theoretically justified mechanism for microseepage, it also shows why interpretation of surface microseepage signals is problematic. Fracture geometry controls seepage velocity and flux, so geochemical anomalies may indicate an increase in fracture aperture, as well as possible subsurface accumulations. Larger fractures require very low gas capillary entry pressures, so in some settings, surface seepage could result from fractures over stratal migration pathways, as well as over petroleum accumulations.

INTRODUCTION

For years, various techniques have been proposed for locating subsurface petroleum accumulations by direct or indirect evidence of petroleum microseepage. Microscopic seeps (microseeps) are seeps of petroleum too subtle to be identified by direct observation but that can be characterized by geochemical means (Price, 1986). Although pervasive microseepage is characteristic of some petroleum basins (e.g., Klusman and Jakel, 1998), in some settings, microseepage forms hydrocarbon anomalies directly above petroleum accumulations. This type of microseepage is commonly explained by

Manuscript received June 21, 1999; revised manuscript received March 9, 2000; final acceptance March 15, 2000.

AUTHOR

ALTON BROWN ~ *ARCO, 2300 West Plano Parkway, Plano, Texas 75075; abrown@arco.com*

Alton Brown has worked with the exploration research group at ARCO for the last 20 years on various topics of carbonate sedimentation and diagenesis, petroleum migration, hydrodynamics, and inorganic gas geochemistry. He is now retired.

ACKNOWLEDGEMENTS

ARCO is gratefully acknowledged for release of this article. I thank ARCO reviewers Mark McCaffrey, Paul Willette, and Ron Gajdica for help with clarity and scope. I also thank AAPG reviewers Alain-Yves Huc, Ronald Klusman, and Peter Gretner for constructive reviews of the original manuscript.

rapid, vertical migration of gas through microfracture networks as colloidal-size gas bubbles (e.g., Saunders et al., 1999). Colloidal gas migration was first proposed by MacElvain (1969). Price (1986) modified the MacElvain model by proposing that the colloidal bubbles migrate up microfractures.

Although the microbubble ascent mechanism has been widely cited, its quantitative characteristics have not been theoretically investigated. Even MacElvain's studies were entirely qualitative in nature. Without a more quantitative analysis of flow rate, whether the mechanism is valid and to what extent fractures are necessary for the leakage process is unclear. If fractures are necessary to provide migration pathways, then geochemical anomalies may be an indication of fractures rather than an indication of a deep hydrocarbon accumulation. If fractures are large enough, surface microseepage could be caused by gas leaking from petroleum migrating in carrier beds, as well as from trapped petroleum. If fractures are pervasive, can any barrier prevent microseepage from accumulations? Is it even possible to trap gaseous petroleum for geological lengths of time if microfractures penetrate the seal of an accumulation?

To address these questions, I quantify the velocity and flux (volumetric flow) of gas bubbles ascending through vertical fractures and compare them to the velocity and flux calculated for continuous-phase gas flow through fractures, the most probable mechanism for focused, vertical cross-stratal migration and macroseepage. I also compare velocities calculated by both mechanisms to velocities reported for microseepage in the literature to see if either mechanism can provide the combination of rapid velocity and low flux proposed for microseepage.

PREVIOUS WORK ON MICROSEEPAGE MECHANISMS

Link (1952) distinguished seeps, in which liquid or gaseous hydrocarbons can still be seen, from microseeps, which must be detected by geochemical or other means. In some cases, microseepage is concentrated directly above petroleum (oil and gas) accumulations as either an edge leakage anomaly or an apical anomaly (Saunders et al., 1999). This implies that the microseepage causing surface anomalies must be vertically focused. Considerable evidence also indicates that microseepage is relatively fast. Production from petroleum accumulations or pressurization of oil pools during secondary recovery changes the surface geochemical anomaly within a few years (Tedesco, 1999; also discussed in a following section). The characteristics of vertical migration through heterogeneous strata and rapid flow rate seem at first glance to be inconsistent with recognized processes of subsurface flow, so many exploration geologists discount the validity of surface geochemical data for localizing petroleum accumulations (Saunders et al., 1999).

Price (1986) summarized the data and previous theories on microseepage mechanisms to try to identify a flow regime that would explain the rapid, vertically focused flow necessary to create microseepage anomalies localized above petroleum accumulations. He identified and analyzed the four mechanisms for migration described in the literature up to that time: (1) diffusion, (2) effusion, (3) advection with moving waters, and (4) permeation. He also proposed a fifth mechanism, colloidal bubble ascent.

Diffusion is a well-documented physical process that undoubtedly contributes significantly to the pervasive microseepage out of some petroleum basins (Leythaeuser et al., 1982). Estimated methane diffusive flux over petroleum accumulations is on the order of 0.1 to 63 kg $CH_4/km^2/yr$ (Krooss and Leythaeuser, 1996). However, diffusion is a slow process that requires millions of years to reach the surface (Krooss and Leythaeuser, 1996), so the rapid changes in surface geochemical signature are inconsistent with a diffusive mechanism. Also, diffusion could not be focused into strong, localized anomalies similar to those reported in the literature (Price, 1986).

The process of effusion is interpreted in the migration context by Price (1986, p. 248) to mean gas flow as an immiscible fluid through water-saturated pore spaces. In matrix porosity, flow is described by multiphase Darcy's law. In fractured rocks, flow is described by a fracture flow law such as that of Huitt (1956). Because flux is coupled to velocity by porosity and saturation, Price (1986) interpreted that effusion having velocity similar to that described in the microseepage literature would result in a flux too great for microseepage; microseeps would actually be macroseeps if this mechanism were operative. For example, Arp (1992a) calculated that vertical microseepage at a velocity of 76 m/yr requires an effective permeability of 11 md. This effective permeability greatly exceeds the absolute permeability of matrix pore networks in fine-grained rocks comprising most of the sedimentary record of typical petroleum basins, so

Arp (1992a) recognized the necessity of fracture porosity for effusion. He limited the total flux of methane leaking from a field to about 7 L CH_4/yr by decreasing the cross-sectional area over which leakage occurs to approximately 1 mm^2. Loss over a square meter increases loss rate by a factor of a million, substantiating Price's (1986) concern on flux rates in matrix pore systems.

Multiphase flow in matrix porosity also requires that the nonwetting phase have sufficient capillary pressure to invade the pore network. The capillary displacement pressures for gas in sealing lithologies such as shales and claystones are commonly greater than 1 MPa (145 psi) and may exceed 10 MPa (1450 psi; e.g., Yang and Aplin, 1998). This exceeds the capillary pressure of most gas and oil accumulations, so the seals cannot be invaded, and leakage does not occur through the matrix porosity. If leakage were to occur through a weak seal, the variations in capillary displacement pressure in interbedded sandstones and claystones overlying an accumulation would constrain the nonwetting phase to migrate parallel with bedding in an updip direction, and the anomaly would not be localized over the accumulation.

Advection with moving waters was eliminated from consideration by Price (1986) because it requires significant vertical water movement to create microseepage anomalies, and such resurgent water is not characteristic of many field locations. Water flow also cannot account for the fast vertical migration velocity (Price, 1986; Klusman and Saeed, 1996). Permeation is dismissed by Price (1986) as a vague term that means either diffusion or gas-phase movement through pore spaces, a process that Price calls effusion.

Price (1986) also considered the colloidal bubble mechanism of MacElvain (1969). MacElvain (1969) was originally concerned with the general problem of gas migration, not just microseepage. At that time, it was not widely realized that gas, like oil, migrates primarily as a continuous, nonwetting phase in a water-wet rock (as described, for example, by England et al., 1987). MacElvain considered only the processes of diffusion and small bubble migration. Like Price, he eliminated diffusion due to slow rates, so he focused on migration of gas as dispersed, small bubbles. He reported qualitative experiments in which large gas bubbles stick to surfaces and are trapped at pore throats. MacElvain proposed that if bubbles were colloidal in size, Brownian motion would prevent them from sticking to surfaces, so they could continue to migrate upward. To demonstrate this mechanism, MacElvain generated colloidal bubbles electrolytically and measured their rate of ascent as several millimeters per second in open water.

Price (1986) concluded that colloidal bubble migration has the desired combination of rapid vertical velocity and relatively low flux that is consistent with microseepage phenomena. However, he further recognized the problem of moving colloidal-size bubbles through the small pore throats of tight shales, so he modified MacElvain's (1969) model by proposing that the colloidal gas bubbles migrate up microfractures. Price further proposed that rocks in sedimentary basins are pervasively microfractured, so pathways to vertical migration are always available to colloidal-size bubbles. The microfractures are large enough for colloidal gas bubbles to migrate yet too small for significant bulk flow of gas. This prevents the effusion that would lead to macroseepage and breached traps. Neither Price nor MacElvain quantified their calculations or experiments. Klusman and Saeed (1996) attempted to model migration of isolated gas bubbles; however, their constitutive equations describe standard multiphase Darcy's Law flow through a porous medium as modeled by most petroleum engineers. The model actually calculates effusive flow.

Although the problem of ascension of gas bubbles in free liquid and fractures has not been specifically addressed in the petroleum geology literature, the physics of the process are very well described in the fluid mechanics literature. Where bubbles are small, bubble ascent is identical with the process of settling of rigid spheres in viscous fluid, only buoyancy results in upward movement rather than downward movement. Following this line, I investigate the theory of bubble ascension in the following sections.

BUBBLE ASCENT

Darcy's law does not apply to ascending bubbles. There can be no definition of gas relative permeability as a function of saturation for discontinuous gas phases, because the saturation is not controlling bubble movement. Bubble ascent can be evaluated by considering four different controls on its velocity: (1) properties of the sphere and the surrounding fluid (ascent of spheres in an infinite viscous medium), (2) effects of walls on bubble ascent, (3) effects of concentration on bubble ascent relative to surrounding water, and (4) effects of concentration on ascent of a mass of bubbles and entrained water.

A sphere moving through a viscous fluid achieves a terminal velocity when viscous forces of drag balance the body force driving movement. Because the bubbles being considered are colloid to micron size, conditions for flow are laminar for all cases of interest. Drag in water is so high that momentum is ignored for small gas bubbles, and the bubble very abruptly approaches terminal velocity for its radius and surrounding fluid viscosity. The body force is the buoyancy effect caused by the density difference between the fluid and the sphere in a gravity field. If the sphere is less dense than the surrounding fluid, the sphere ascends.

The analysis presented in this article compares velocity and flux under identical conditions, so the gas is considered incompressible. Real gas bubbles are highly compressible, so their radius changes significantly with depth, especially near the surface (see the Effects of Pressure section). However, pressure affects all bubbles equally, so compressibility effects on relative motion can be ignored for issues of relative velocity. Although Brownian motion is essential for the MacElvain model, it also is ignored in this analysis, because over time the changes in velocity due to Brownian motion cancel one another.

Stokes' Velocity

In an infinite viscous medium having no walls or other particles, Stokes' law describes the bubble terminal velocity, because the bubbles are spherical and the Reynolds number (Re) for very small spheres is much less than one. The terminal Stokes' velocity (U_s) is

$$U_s = \frac{2a^2(\sigma - \rho)g}{9\mu} \qquad (1)$$

where a is the particle radius; σ and ρ are the densities of the sphere (gas bubble) and fluid (water), respectively; g is acceleration due to gravity; and μ is the viscosity of the water through which the spheres move (Allen, 1984, p. 75). Water viscosity is used rather than gas viscosity, because the water must be deformed and displaced around the rising gas sphere, which maintains it shape during rise.

Wall Effects

Proximity to walls decreases terminal velocity. Buoyancy is unaffected by the proximity to a wall, but viscous drag increases. The fluid displaced by the rising sphere is squeezed into a narrower cross sectional area between the wall and the particle, which increases the viscous resistance to flow and slows the sphere. Movement of bubbles in a vertical fracture of constant aperture can be approximated by sphere motion between parallel plates. The relative decrease in velocity due to increased drag is a function of the position of the particle between the walls and the ratio of the particle radius to the aperture between the parallel plates (Happel and Brenner, 1965, p. 322–328). Fastest normalized velocity is halfway between the two walls. Wall effects decrease as the ratio of the sphere radius to half width separating the plates decreases. For a sphere of radius a rising halfway between parallel plates separated by a width (aperture) of 2ℓ, the terminal velocity normalized to the Stokes' velocity for the same radius sphere can be approximated by the following equation:

$$\frac{U}{U_s} = 1 - 1.004(a/\ell) + 0.418(a/\ell)^3 - 0.21(a/\ell)^4 - 0.169(a/\ell)^5 \qquad (2)$$

This equation is modified from equation 7–4.27 in Happel and Brenner (1965, p. 327), having the sign of the second reflective term ($(a/\ell)^4$) corrected to negative from positive, following the sign of similar reflective terms in their equations 7–4.25 and 7–4.28.

Wall effects are smaller for particles significantly smaller than the aperture between parallel plates (Figure 1). For a given fracture aperture, the sphere radius must decrease to decrease wall effects. However, as the sphere radius decreases, its Stokes' terminal velocity decreases. The total velocity reaches a maximum at a ratio of the sphere radius to fracture half width of 0.74. Likewise, the radius at which volumetric flux is maximized can be calculated as 0.88 times the fracture half width (Figure 2). The volumetric flux of a bubble ascending between parallel plates is the product of its velocity and volume. Although bubbles having radius greater than 0.74 times the half width may move more slowly, their total flux may be greater owing to their larger volume.

If natural fractures are not exactly vertical, buoyancy of the bubble results in the bubble migrating as it touches the upper wall of the fracture. In this position, frictional drag is maximized and velocity minimized for the given radius/half width ratio. The estimate provided by equation 2 is the fastest bubble ascent velocity that can occur in a fracture, and this

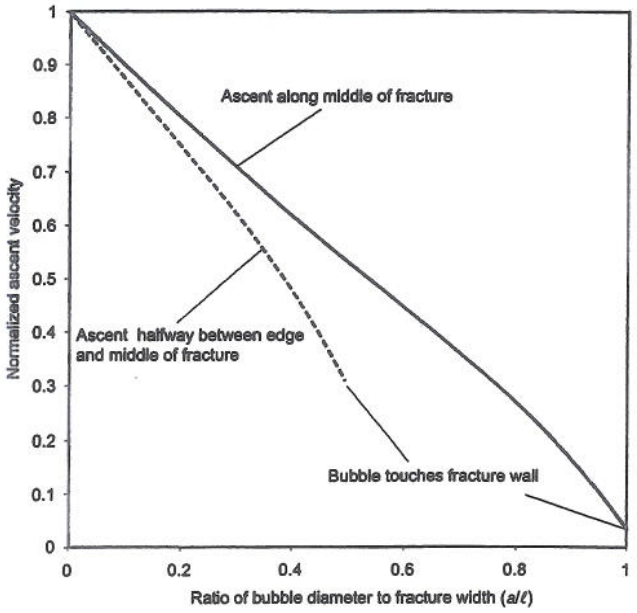

Figure 1. Velocity of a sphere ascending between parallel plates as a function of the ratio of bubble radius to the fracture half width. Velocity is normalized to Stokes' velocity. Solid curve is the terminal velocity for particles rising halfway between parallel plates. The dashed line is the terminal velocity for particles rising half way between the middle and one of the walls. Wall effects are minimized where the sphere radius is infinitesimal.

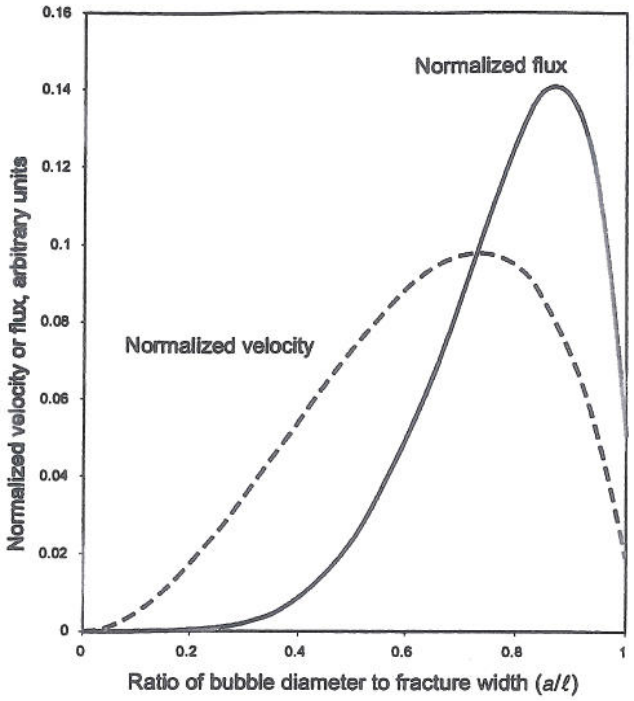

Figure 2. Normalized velocity and flux of bubbles ascending between parallel plates as a function of the ratio of the bubble diameter to the fracture width (a/ℓ). Velocity and volumetric flux are normalized to arbitrary units.

velocity can only be achieved where the fracture is exactly vertical.

Concentration Effects

As the concentration of particles in a fluid increases, particles interfere with each other's ascent. Therefore, terminal velocity decreases relative to surrounding water as concentration increases. The velocity decrease relative to the zero-concentration velocity (U^*) is described by the following relationship (Churchill, 1988, p. 542–545):

$$\frac{U_c}{U^*} = (1 - C)^n \qquad n = 4.65 + 20\,\frac{a}{a_t} \qquad (3)$$

where $Re < 0.2$. C is the volume fraction concentration of spheres, a is the sphere radius, and a_t is the radius of the tube through which the particles are rising (approximately equivalent to 2ℓ for ascent between parallel plates). The exponent n is entirely a function of the normalized particle diameter at low Reynolds numbers ($Re < 0.2$), but at higher Reynolds numbers, n decreases with increasing Reynolds numbers (Churchill, 1988, p. 542–545). A Reynolds number of 0.2 corresponds approximately to a bubble radius of 50 μm in water, so the Reynolds number for the much smaller bubbles of interest is much smaller than 0.2. The concentration effect described by equation 3 can be combined with the wall effects by multiplying the two terms. For bubble ascent in fractures, the reference velocity (U^*) is the bubble terminal velocity in a fracture described by equation 2. For uniform spheres, the maximum sphere concentration is around 45%, corresponding to random, nontouching packing. Velocity is retarded to about 5% of the free rising velocity for very small bubbles at this maximum concentration (0.45; Figure 3).

The second effect of bubble concentration is to decrease the bulk density of the fluid containing the bubbles, so that the entire mass (bubbles and entrained water) rises relative to both surrounding water without gas bubbles and fracture walls. This type of motion falls into Allen's (1984, p. 84) class IIIb sediment dispersion, because particle–fluid and particle–particle interaction is significant. Analogous flows in natural settings are various sediment gravity flows, such as turbidity currents. However, the microfractures discussed here,

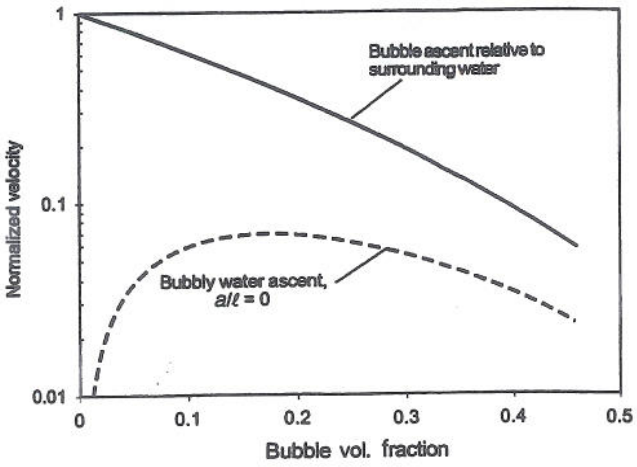

Figure 3. Effects of concentration on ascent velocity. Bubble velocity relative to surrounding water (solid line) was calculated from equation 3 using $n = 4.65$ (infinitesimal bubble radius). Velocity is normalized to Stokes' velocity. Velocity of a bubbly water mass in a fracture (dashed line) was calculated from equation 5 using effective viscosity calculated from equation 4 and assuming an infinitesimal bubble radius. Bubbly water velocity is normalized to Stokes' velocity of a bubble having diameter equal to the fracture width. Because the two velocities are normalized to different quantities, their relative velocity cannot be compared using this figure. See Figure 5 for the comparison.

through which bubbly water must flow, are so small that flow is laminar. This means that particle interaction or turbidity cannot stabilize the mixture, so the suspension always decomposes. As noted by Churchill (1988, p. 551), as long as bubble diameters lie within a 6:1 ratio of each other, a sharp interface is maintained by the rising bubbles separating the bubbly water from surrounding bubble-free water. This means that in bubbly water, two velocities have to be considered, the velocity of the bubbly water mass (bubbles and entrained water) and velocity of the bubbles within the bubbly water mass. Total gas bubble velocity is the sum of the two.

Movement of a bubbly water mass up a fracture can be described by the continuous-phase flow between parallel plates discussed in a following section (equation 5). Buoyancy provided by bubbles increases linearly with increasing bubble concentration. However, as bubble concentration increases, the effective viscosity of the fluid increases, because the bubbles act as solid, nondeformable beads that restrict the flow of fluid. The relationship between increasing buoyancy and decreasing viscosity determines at what concentration the ascent velocity is maximized. The empirical relationship described by equation 3 can be used to estimate the effective viscosity from concentration and bubble size (Brodkey, 1967, p. 630, 633). In a similar manner, the effective viscosity due to the presence of fracture walls can be estimated from equation 2. This underestimates average effective viscosity, because higher effective viscosity near the fracture walls is not considered. The resulting effective viscosity is a function of water viscosity (μ_w), concentration (C), sphere size (a), and fracture half width (ℓ):

$$\mu_e = \mu_w [(1 - C)^{-n}] \div [1 - 1.004(a/\ell) + 0.418(a/\ell)^3 - 0.21(a/\ell)^4 - 0.169(a/\ell)^5] \quad (4)$$

where $n = 4.65 + 10a/\ell$ at $Re < 0.2$. For purposes of modeling bubbly water ascent up fractures, it is assumed that the bubble suspension is stable for the duration of flow and has a viscosity that is controlled by equation 4. For infinitesimal bubble size ($a/\ell = 0$), velocity maximizes at a concentration of 18% bubbles (Figure 3). At higher concentrations, greatly increased viscosity retards ascent, whereas at lower concentration, buoyancy is less.

CONTINUOUS GAS-PHASE FLOW IN FRACTURES

Gas migration is believed to occur mainly as a continuous gas phase in the rock or at least as a body of gas very much larger than a single pore or pore throat (England et al., 1987). Fractures having constant apertures become essentially completely saturated with gas once invading gas exceeds the capillary displacement pressure of the fracture. Idealized flow of gas in fractures can therefore be described by a single-phase flow relationship. Single-phase flow in a fracture can be approximated by flow between parallel plates. For a fracture width W (Huitt, 1956)

$$\text{velocity}(U_f) = \frac{W^2}{12\mu}\frac{dP}{dz} = \frac{4\ell^2}{12\mu}(\sigma - \rho)g \quad (5)$$

$$\text{flux}(q/L) = \frac{W^3}{12\mu}\frac{dP}{dz} \quad (6)$$

where U_f is velocity of fluid in the fracture perpendicular to width, μ is viscosity, dP/dz is the vertical excess pressure gradient, q is the volumetric flux, and L is unit

length of fracture measured perpendicular to the flow direction, z. For comparison to equation 1, equation 5 is rewritten in terms of fracture half width, $\ell = W/2$, and the pressure gradient is chosen to be that of buoyancy-driven flow, $(\sigma - \rho)g$ (consistent with the assumption that the gas is leaking from a normal-pressured reservoir at depth). For gas migration in the fracture, gas viscosity and density are used. For the case of bubbly water, viscosity of the bubbly water mass is calculated from equation 4, and its density is calculated from the volume fraction of gas bubbles in the water.

The stability of motion of the bubbly water can be determined in part by the Reynolds number. Generally, as long as the Reynolds number remains less than about 1000, flow between parallel plates remains laminar (Huitt, 1956). Under laminar conditions, bubbles can separate from the water, so bubble concentration changes during ascent; that is, flow is unstable. The Reynolds number for flow through fractures is $2WU_f\rho/\mu$ (Huitt, 1956), and the velocity (U_f) is a function of width. Because the approximate fracture width at which turbulent flow initiates is in excess of a millimeter for bubbly water, bubbly water ascent in microfractures is unstable.

MIGRATION VELOCITY

Calculated Gas Migration Velocity by Different Mechanisms

Reference conditions of 37.8°C and 10.3 MPa (100°F and 1500 psi) were chosen to compare the velocity of the different transport mechanisms under the same physical conditions. These conditions correspond to an approximate subsurface depth of 1055 m (3500 ft) under normal pressured conditions. Table 1 lists properties of fluids at these conditions. Because shallow pore pressures are commonly near hydrostatic, the migration of the gas phase does not modify the fracture aperture. Thus, the fracture apertures are considered fixed for these calculations. The fluid potential gradient for fracture flow is assumed to be that of buoyancy caused by density difference between gas (or bubbly water) and water. This approximates the conditions of a normally pressured gas reservoir having a relatively thin gas column. A "water drive" assumption is made; that is, water replaces lost gas so that gas pressure in the leaking reservoir remains approximately the same during leakage. Under these conditions, gas fracture flow remains laminar up to a fracture width of 112 μm, and bubbly water fracture flow remains laminar up to at least 1 mm fracture width.

Figure 4 compares velocity of gas migrating by 4 mechanisms: (1) continuous-phase gas migrating in fractures, (2) bubble ascent without wall or concentration effects (Stokes' law), (3) maximum velocity of isolated bubble ascent in fractures, and (4) steady ascent of bubbly water in a vertical fracture having infinitesimal bubble size and 18% gas concentration (maximum ascent velocity; Figure 3). The horizontal axis is either the bubble radius (for Stokes' law terminal velocity) or the fracture half width (for maximum bubble velocity in fractures, continuous gas-phase flow, and bubbly water flow).

The ascent velocities by the four mechanisms form parallel lines, indicating that the relative velocity of the mechanisms does not change with fracture or bubble size. Continuous-phase gas migration is the fastest, followed by free bubble ascent and bubble ascent in fractures. Bubbly water ascent is the slowest

Table 1. Assumed Fluid Properties

Property	Petroleum Engineering Units	SI Units
Water density	0.996 g/cc	996 kg/m^3
Water viscosity	0.89 cp	0.00089 Pa·s
Gas density	0.1 g/cc	100 kg/m^3
Gas viscosity	0.015 cp	0.000015 Pa·s
Water-gas surface tension	72 dynes/cm	0.072 N/m

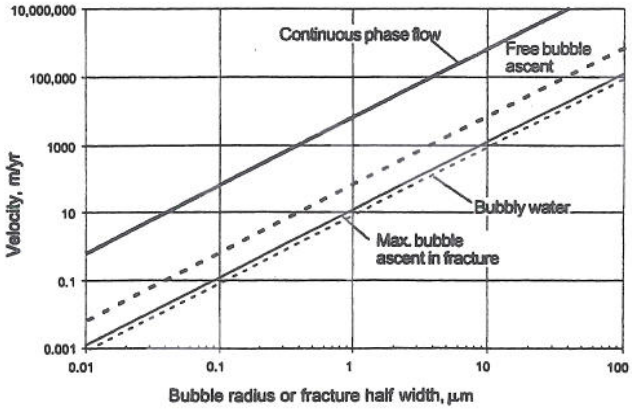

Figure 4. Gas ascent velocity by different mechanisms as a function of bubble radius or fracture half width. Laminar flow is assumed.

mechanism, even under the most favorable conditions.

The constancy of the ratios between velocities of different transport mechanisms under the modeled conditions is caused by fundamental relationships between the various equations describing velocity. If equation 1 is divided by equation 5, the ratio of terminal velocity for a freely ascending bubble to velocity of continuous gas-phase migration buoyantly ascending in a fracture having half width equal to the bubble radius entirely depends on the relative viscosities of gas and water:

$$\frac{U_s}{U_f} = \frac{2\mu_g}{3\mu_w} \qquad (7)$$

The viscosity of single-phase gas flow in a fracture is that of the gas. The viscosity controlling bubble ascent in a fracture is that of water, because water must move aside as the bubble ascends. The viscosity of water is about 60 times that of gas under conditions assumed in Table 1, so continuous-phase flow in fractures is approximately 90 times faster than free bubble ascent, regardless of the fracture half width.

Because bubble radius necessary for maximum velocity in a fracture is 0.74 times the fracture half width, maximum fracture bubble velocity is fixed relative to free bubble velocity. Maximum ascent velocity in a fracture is only 0.326 times the free ascent velocity of a bubble of equal radius. Because the bubble radius is smaller than the fracture half width, the total maximum bubble velocity in a fracture is about 18% of the velocity of a freely ascending bubble having radius equal to the fracture half width.

Bubbly water velocity is harder to characterize, because bubble concentration and radius control the ascent. Also, the ascent velocity is the sum of the bulk movement of the bubbly water and the movement of the bubbles within the bubbly water mass. To compare the effects of these two mechanisms, concentration and bubble radius relative to fracture width were varied and the ascent velocity compared (Figure 5). Fastest rise occurs at infinitesimal concentrations and relatively large a/ℓ. As concentration increases, maximum velocity decreases and occurs at smaller bubble size. Bubbly water ascent having infinitesimally small bubbles dominates flow at concentrations greater than about 10%, but total ascent velocity is much less than that of isolated bubble ascent at infinitesimal bubble concentration. At bubble concentrations higher than 0.18, the ascent velocity decreases with increasing concentration owing to increased effective viscosity.

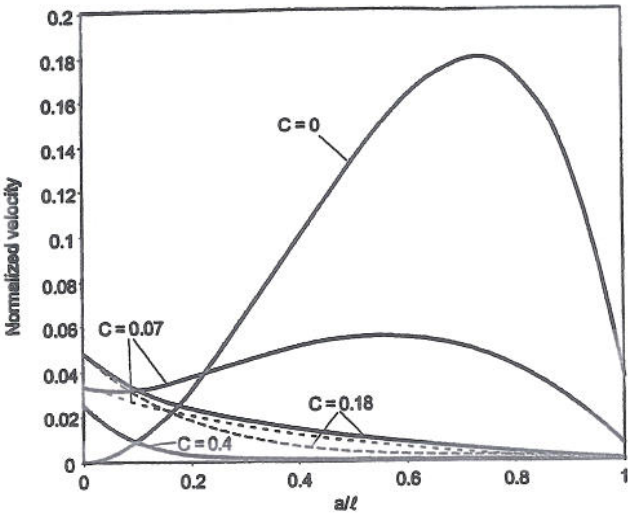

Figure 5. Effect of bubble concentration (C) and bubble radius normalized to fracture half width (a/ℓ) on ascent velocity of bubbly water. Mass ascent of bubbly water is shown by thin dashed lines, and total gas ascent velocity (sum of bubbly water velocity plus velocity of bubbles in water) is shown by solid lines. At low concentrations, individual bubble velocity dominates, so velocity peaks at larger bubble size. At high concentrations, bubbly water velocity dominates, so maximum velocity is at small bubble size. Velocities are normalized to Stokes' terminal velocity of a bubble having diameter equal to the width of the fracture through which bubbly water is migrating.

Comparison to Seepage Velocity

Seepage velocity has been estimated by evaluating the effects of subsurface pressure changes on surface geochemical signatures (Table 2). Most data are collected over gas storage sites or over producing reservoirs. Most reported rates are on the order of 100–10,000 m/yr. Slower velocities are based on time increments between isolated surveys, so faster velocities are probably more valid. However, the fastest velocities are not measured in natural accumulations, so these rates may exceed those over natural accumulations. Other examples have artificially raised pressures that may enhance migration rates. However, rates of approximately 100–1000 m/yr agree with the large body of qualitative literature documenting changes in geochemical signatures a few years after initiation of production (e.g., Tucker and

Table 2. Gas Seepage Velocity

Reference	Facility	Velocity, m/yr	Comments
Arp, 1992b	Patrick Draw field, WY	76.3–305	
Jones and Burtell, 1996	Rock Springs coal gasification	32,850	Fumes generated by subsurface burn
Jones and Burtell, 1996	Gas storage seepage	1460	
Horwitz, 1969	Hastings field, TX	>100	Geochem. surveys separated by 22 yr
Araktingi et al., 1984	Leroy gas storage, CO	1370	Leakage associated with fault

Hitzman, 1996; Schumacher et al., 1997; Tedesco, 1999).

Even under the most favorable assumed conditions, the migration of isolated gas bubbles up fractures is too slow to account for observed seepage velocity, so this hypothesis must be abandoned. At their fastest velocity, colloidal-size (radius < 0.12 μm) bubbles move up fractures at less than 1 m/yr (Figure 6). This value rules out colloidal bubble migration, because this calculated seepage velocity is so much slower than observed rates. Under MacElvain's (1969) hypothesis, Brownian motion controls maximum bubble size that migrates. Therefore, the maximum bubble size for this mechanism is the maximum size at which Brownian motion is observed, a radius of about 2.5 μm. However, even at this larger size, individual bubble migration rates up fractures are less than 100 m/yr, so isolated bubble migration cannot explain observed gas seepage velocity. Although individual bubbles ascend in free water at rates sufficient for the lower part of the observed seepage velocities, wall effects must occur in fractures, so terminal velocities calculated by Stokes' law cannot occur during subsurface seepage.

Single-phase gas flow in small fractures is consistent with the rapid seepage velocities reported in the literature. Fractures having half widths from 0.1 to 2 μm can be responsible for buoyancy-driven flow at rates equal to the range of reported seepage velocity (Figure 6).

Under the most favorable conditions for bubbly water migration (C = 0.18, a/ℓ = 0), the observed rates of migration can be achieved only if large fractures are assumed. To match the highest observed seepage velocity, fracture half widths of 50 μm or more must be assumed. Of course, even higher velocity by continuous gas-phase flow is possible in these large aperture fractures.

ENERGETICALLY FAVORABLE MECHANISMS

The formation of gas bubbles or gas-filled fractures requires that the gas pressure exceed the pressure of the surrounding liquid by a pressure sufficient to overcome the surface tensions created by introducing a new phase. This pressure is the capillary pressure. It acts as a threshold for motion because neither gas bubbles nor gas filling fractures can migrate until the gas phase forms. If one transport mechanism requires lower capillary pressure and if the rates of transport at that capillary pressure are sufficiently high, then pressure does not rise high enough to activate other transport mechanisms. The mechanism requiring the lowest capillary pressure for migration is the most energetically favorable, because the least amount of pressure is required to activate it.

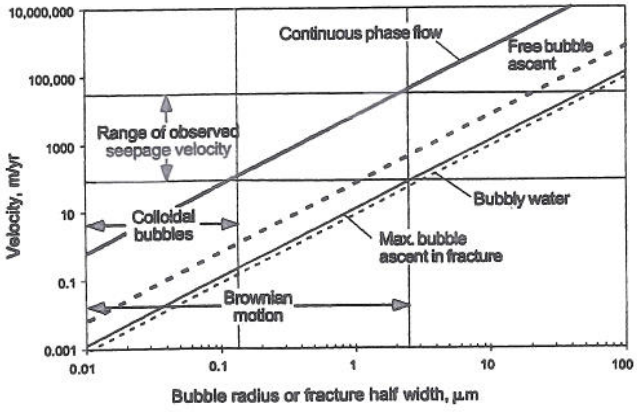

Figure 6. Comparison of calculated migration velocities for proposed mechanisms and observed seepage velocities. Over the range of bubble radii where Brownian motion could occur, bubble migration is significantly less than observed seepage velocity. In contrast, gas migration as a continuous phase in fractures can easily migrate this fast at very small fracture apertures.

Capillary pressure (P_c) is inversely related to bubble radius by twice the surface tension (γ; equation 8). Capillary pressure between infinite parallel plates is inversely proportional to the half width of the fracture (ℓ; equation 9):

$$\text{Spheres: } P_c = \frac{2\gamma}{r} \tag{8}$$

$$\text{Parallel plates: } P_c = \frac{\gamma \cos \theta}{\ell} \tag{9}$$

Capillary pressure of gas bubbles in water is not affected by wettability, because the bubbles do not come into contact with the rock surface. In contrast, the shape of the gas phase invading a fracture is controlled by the parallel plates, so wettability (as cosine of the contact angle measured through the water phase, θ) may decrease the capillary pressure. Generally, gas-bearing rocks are strongly water wet, so the cosine of the contact angle is near 1. If completely water-wet conditions are assumed, the capillary pressure needed to invade a fracture is half that needed to form a bubble having a diameter equivalent to the fracture width (Figure 7). If the rock is partially wetting to the gas phase, then capillary pressure needed to invade the fracture is even less.

Because gas requires only half the capillary pressure to invade fractures as would be required to form a gas bubble of equivalent diameter, it is energetically easier for gas to invade fractures as a continuous sheet-like phase than as isolated bubbles. Maximum velocity of isolated bubbles in fractures requires that bubble radius be smaller than the fracture half width, so the capillary pressure needed for most rapid bubble migration is more than a factor of 2 greater than that required for continuous gas-phase flow in a fracture.

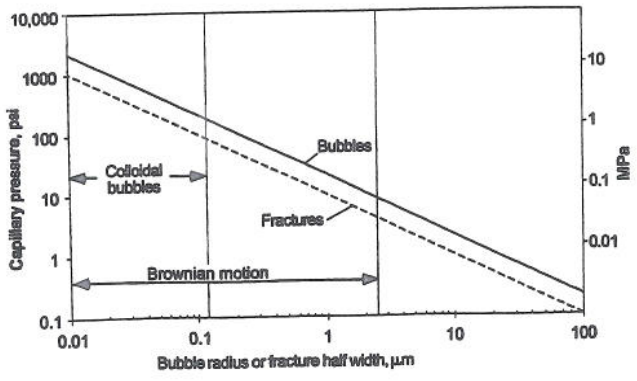

Figure 7. Gas-water capillary pressures of bubbles (solid line) and fracture-filling gas (dashed line) as a function of bubble radius or fracture half width. Totally water-wet conditions and a surface tension of 72 dynes/cm are assumed.

Invasion of bubbly water into fractures requires no surface tension. However, the colloidal-size bubbles that constitute the gas fraction of the bubbly water mass require considerable capillary pressure to form, on the order of 1.4 MPa (200 psi) or greater (Figure 6). Under typical subsurface conditions, this would require a gas column more than 150 m (500 ft) thick. Such thick gas columns occur in giant fields but not in the many smaller fields having documented surface seepage. Formation of a bubbly water mass having colloidal-size gas bubbles would be difficult or impossible without adequate capillary pressure in the underlying reservoir. For this reason, bubbly water ascent is not only slow but essentially impossible to initiate in thin petroleum columns.

MIGRATION FLUX

The volumetric flux can be readily calculated for any of the mechanisms evaluated in this article using simple modifications to the velocity equations discussed previously. The same conditions assumed for the velocity models are used. However, the results are reported in units of mass flux.

The fastest and energetically most favorable mechanism, continuous gas-phase flow through fractures, shows a tremendous flux change with fracture aperture consistent with its cubic relationship (equation 6). A fracture having a half width of 0.1 µm at conditions assumed in Table 1 delivers about 0.01 g CH_4 per linear meter of fracture per year, whereas a fracture having a half width of 10 µm could deliver 10 kg per linear meter of fracture per year (Figure 8). The average methane flux measured by Klusman and Jakel (1998) of about 200 kg $CH_4/km^2/yr$ for the Denver-Julesburg basin is used to determine fracture spacing for varying fracture half widths at 1 km depth. Fractures having 0.1 µm half width would have to be spaced at 4.8 cm apart to account for the observed flux. Fractures having 1 µm half width would be spaced at 48 m apart, and fractures having 10 µm half width would be spaced 48 km apart to explain the same average flux. By varying the combination of fracture width and fracture spacing, the flux can be made arbitrarily high or low, rang-

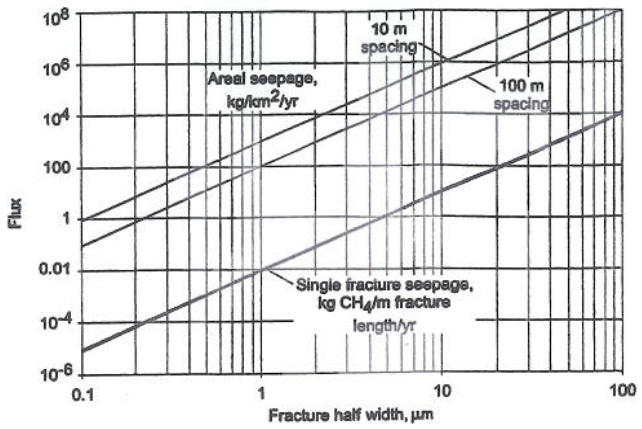

Figure 8. Gas flux due to continuous-phase flow in fractures. Heavy line is kilograms of gas migrated per meter length of fracture perpendicular to flow direction per year. The two thin lines are areal fluxes, assuming a 10 m fracture spacing (upper line) and 100 m fracture spacing (lower line).

ing from essentially undetectable microseepage to macroseepage. In all cases having reasonable gas flux, the average fracture porosity is negligible.

Because the geometry of fracture flow is fixed, the ratio of flux to velocity for motion up a given fracture is fixed by the width of the fracture and the concentration of gas in the moving medium. Because the bubbly gas has only 18% gas at its maximum velocity, its flux is only 18% of the flux of a continuous gas phase at an equivalent migration velocity. Continuous gas-phase velocity is about 830 times faster than the fastest bubbly water velocity, so in equivalent width fractures, gas flux in bubbly water is about 0.022% that of gas migrating as a continuous phase through the same width fracture. Maximum gas flux can also be calculated for isolated bubble migration. I determined by trial and error that the maximum flux for bubble ascent occurs at a/ℓ of 0.65 and concentration of 0.055, where the flux is 0.00355% that of gas migrating as a continuous phase through the same width fracture.

DISCUSSION

Mechanism of Localized Gas Microseepage

Up to this point, I have considered idealized short segments of fracture migration pathways consisting of fractures having parallel vertical walls. The purpose for this simplification was to demonstrate that under fixed geometric constraints, bulk gas fracture flow is much faster and energetically more favorable than migration of gas as isolated microbubbles. Although specific viscosities and densities were chosen to illustrate this in Figure 4, continuous gas-phase flow in fractures is so much faster than any of the gas microbubble mechanisms that any reasonably chosen conditions yield similar results. Based on these results, it seems reasonable to conclude that microbubble ascent is much less effective for focused gas microseepage than continuous gas-phase migration in fractures.

Continuous gas-phase migration in fractures can leak at the reported seepage velocities, but the original objection to this mechanism is that the flux rate would be too high. If leakage rate is too high, gas accumulations are not preserved long enough to be discovered. Macgregor (1996) determined that the median age of giant, gassy oil accumulations was about 35 Ma, and that destruction of most petroleum accumulations was caused by petroleum destruction or macroseepage. However, some oil and gas accumulations are hundreds of millions of years old (Brown, 1999). Microseepage rates must be low enough to preserve accumulations for tens to hundreds of millions of years; otherwise, surface geochemical anomalies would indicate where accumulations were, not where they are.

Microseepage flux for continuous gas-phase migration can be calculated from equation 6 for different size fractures at an arbitrary fracture spacing if the gas properties are fixed. Of course, gas expansion, viscosity change, fracture spacing, and other effects make this analysis semiquantitative at best, but at least the order of magnitude leakage rate can be estimated. Figure 8 shows the methane mass lost per square kilometer, assuming 10 m-spaced fractures and 100 m-spaced fractures. To determine the approximate fracture aperture and spacing, maximum leakage rate must be estimated for fields of a size similar to those where surface geochemical anomalies are detected. The following conditions are assumed: a gassy oil field (200 m^3 gas/m^3 oil) having a thin oil column (10 m), moderate porosity (20%), and typical oil saturation (80%). Assuming a 40% withdrawal efficiency, this gives an estimate of 128 m^3 CH_4/m^2 gas in the moveable oil. Assuming that half of the gas and oil is lost in the median lifetime of 35 m.y. gives a leakage rate of 1.8 m^3/m^2/m.y., or 1.28 kg/km^2/yr. This leakage rate is very low, especially compared to the background seepage rates of about 200 kg CH_4/km^2/yr for the Denver-Julesburg basin (Klusman and Jakel,

1998). From Figure 8, this leakage rate corresponds to a fracture half width of 0.11 μm at 10 m fracture spacing or 0.24 μm half width at 100 m fracture spacing. Assuming a leakage rate one-tenth of that calculated previously to correspond to a field half-life of 350 m.y., the fracture half widths would correspond to 0.05 and 0.11 μm at 10 and 100 m spacing, respectively. Leakage rates necessary to deplete a gas trap having similar reservoir thickness and properties would be about twice those of the oil accumulation given previously, resulting in negligible change in fracture aperture.

Fracture half widths calculated here are a bit smaller than those corresponding to the average leakage rate but fall within the range of fracture half widths corresponding to observed leakage rates. Capillary displacement pressures for fractures 0.1 to 0.3 μm half width are approximately 0.69 to 0.21 MPa (100 to 30 psi). This corresponds to a gas column approximately 80 to 15 m (260 to 50 ft) high, so most moderate to tall gas columns could invade these small fractures and initiate microseepage.

Based on these first order approximations of leakage flux and capillary pressure needed for leakage, it is possible for gas to seep through fractures by continuous gas-phase flow at rates approximately equivalent to reported surface leakage velocity yet at a flux sufficiently low to allow the trap to be preserved for geological lengths of time. However, the range of fracture widths where both migration velocity is high and flux is low is narrow.

Flow-Path Heterogeneity

Because extremely simplistic fracture geometries and conditions were assumed for the analysis of leakage mechanisms, it is necessary to evaluate the relative effects of these assumptions on migration mechanisms and rates. The biggest assumption is the simple geometry of the migration path: flow between vertical parallel plates. In reality, fractures have dips less than vertical, and aperture changes with position in the fracture. Also unlikely is that a single fracture extends from the reservoir to the surface, so more realistic fracture networks must be considered. Another major effect on flux estimates is the assumption of gas incompressibility. Whereas this may be an acceptable assumption for flow analysis at a fixed depth under steady flow conditions, the gas density and viscosity change substantially with pressure and temperature.

Bubbles rising through a fracture having dip less than 90° migrate against the upper wall. Even if the bubbles do not stick to the wall, the close proximity to the wall results in significantly greater drag and slower ascent velocity. In contrast, lower dip has much less affect on continuous gas-phase flow. The major effect is a decrease in pressure gradient by the sine of the dip angle. This results in a minor velocity decrease in steeply dipping fracture systems.

Real fractures have lateral and vertical variations in aperture. Where the aperture is thin, gas does not fill the fracture owing to insufficient capillary pressure. Otherwise, the width of the fracture controls the width of the gas body. Because width is variable, flux under the constant fluid potential gradient assumed previously would be different in different parts of the fracture. If flow is steady, then the fluid potential gradient must change locally to accommodate changes in width. This results in variation in capillary pressure along the fracture, which results in variable gas saturation. As a result, only part of the fracture is saturated with gas, so total flux is controlled by not only fracture spacing but also variations of aperture within each fracture.

The next step in fracture complexity is the change from a single fracture of variable width to fracture networks. In a way, fracture networks are similar to matrix pore networks. After all, fractures are just highly elongate pores (commonly having a preferred orientation). Both pore systems can be considered percolation networks having the sites being pores (or fracture intersections) and the bonds being the pore throats (or fractures). According to general percolation theory, networks of sites and bonds have a percolation threshold above which flow through infinite networks becomes possible. In porous rocks, this saturation is reached at the capillary displacement pressure for the rock. Because fracture systems are conceptually similar to other pore networks, a threshold saturation or capillary pressure should characterize fracture systems as much as they do other pore systems. Also, saturation of fracture systems varies with the capillary pressure, increasing effective permeability where gas saturation is highest. Because of the size of fracture systems, the capillary displacement pressure cannot be experimentally determined in the lab as can standard porosimetry, but it may still exist in the large scale structure of fracture systems. The pressure valve behavior described by Araktingi et al. (1984) may be caused by these fracture system capillary phenomena. Once this threshold is exceeded, steady flow as described previously is possible.

Effects of Pressure

As gas migrates upward, it is exposed to lower pressures and temperatures. Both density and viscosity decrease as gas volume increases. For gas bubbles, the most significant effect is the increase in bubble radius due to expansion of gas at lower pressure (Figure 9). As the bubble radius increases, bubble velocity in open water accelerates. However, in fractures, the maximum bubble size is limited by the fracture aperture, so increased radius ultimately results in occlusion of the bubble in the fracture. As bubbles occlude, they coalesce to form a larger mass of continuous-phase gas. Once capillary pressure in this mass is sufficient to invade aperture restrictions in the fracture, migration continues as continuous gas-phase migration in the fracture.

Changes in density, viscosity, and gas volume also affect continuous gas-phase migration in fractures. Change in volume overwhelms the minor decrease in viscosity and the minor increase in buoyancy. Assuming an equal width fracture from reservoir to surface, the greater volume needed to flow through fractures at shallow depths requires a steeper fluid potential gradient at those depths. This results in a strongly concave-downward gas pressure vs. depth profile in the fracture (Figure 10). This pressure distribution has not been reported in leaking reservoirs. One possible explanation is that the increase in number of fractures and fracture aperture toward the surface may be able to offset the increased gas volume. Another effect may be a change in gas saturation of a fracture system having increased capillary pressure.

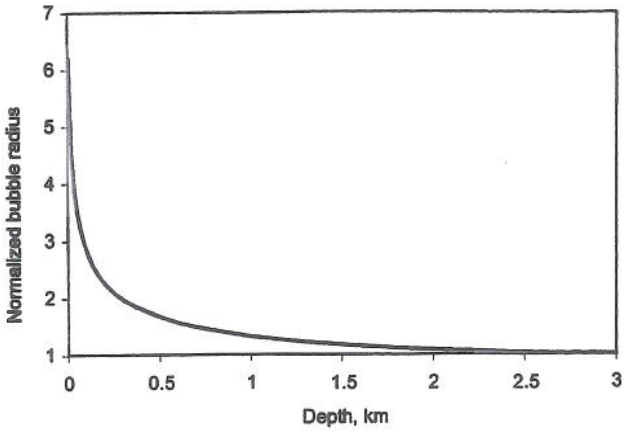

Figure 9. Change in bubble radius as a function of depth, given hydrostatic pressure gradients and 25°C/km thermal gradient. Most change in radius occurs at depths of less than one-half km.

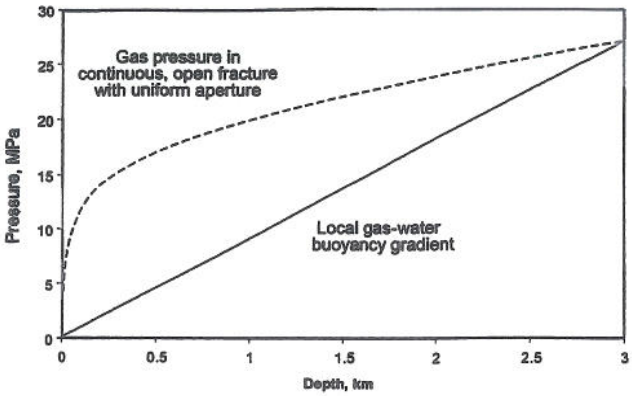

Figure 10. Effect of volume expansion on gas fluid potential vs. depth. The dashed line assumes steady, nonuniform flow of an expanding gas in a fracture of constant aperture, where the pressure at 3 km and surface are externally controlled. The solid line is the local buoyancy gradient for an expanding gas.

Implications for Exploration Geochemistry

The results presented in this article have positive and negative impact on the exploration utility of surface geochemical anomalies. On the positive side, I present a theoretically justified mechanism for surface microseepage. This mechanism can account for the rapid migration velocity reported by surface geochemical methodology yet leak at low enough flux so that gas and gassy oil accumulations can exist for geologically significant time. The effect of tectonic stress on fracture apertures could explain some of the temporal variability (lack of reproducibility) of geochemical anomalies, because flux is extremely sensitive to fracture aperture. Pressure valve effects due to decreased capillary pressure may also explain the rapid and abrupt decrease in some anomalies with petroleum production. The availability of a realistic migration mechanism provides a theoretical justification for the interpretation that surface geochemical anomalies are not just random but instead can serve as evidence of underlying petroleum accumulations.

On the negative side, the narrow range of fracture widths that would allow rapid surface seepage yet prevent significant gas loss implies that the distribution and aperture of fractures may have as much or more influence on distribution of geochemical anomalies than does the distribution of accumulations. Case studies showing that a known field has a geochemical

anomaly may not be sufficient to demonstrate that an undrilled anomaly overlies an accumulation rather than a zone having higher fracture density or wider fracture aperture. Only accumulations overlain by rock having the correct fracture aperture are likely to give a geochemical anomaly, so the absence of an anomaly may not indicate the absence of petroleum. It may also be possible that the ring anomalies commonly observed in geochemical surveys may in some cases result from widely spaced conjugate fracture zones rather than from interaction of leaking petroleum and shallow processes, as is commonly believed (e.g., Saunders et al., 1999). Fracture distribution may also account for the irregular distribution of apical anomalies.

Surface geochemical anomalies may also be legitimate evidence for uneconomic petroleum accumulations or migration pathways. Oil and gas migrating in fine-grained carrier beds could easily invade fracture systems having connected fracture apertures 5 to 10 μm across, because the capillary displacement pressures needed to invade these large fractures is quite low. The result may be a surface geochemical anomaly but no underlying trap or a severely leaking trap. Vertical leakage of migrating oil and gas through widely spaced large fractures could be responsible for distribution of the background geochemical signature of oil seen in cuttings in oil-prone basins, as well as for many of the background hydrocarbon concentrations in surface geochemical studies. After all, macroseepage up fracture zones and faults not directly overlying accumulations is commonly observed in basins actively generating oil and gas. Why shouldn't microseepage behave the same way? If so, how do we distinguish microseeps indicative of accumulations from those indicative of basinal petroleum migration?

CONCLUSIONS

Analysis of several flow mechanisms demonstrates that flow of gas as a continuous phase in fractures can account for the rapid vertical migration velocity reported over accumulations, whereas the previously proposed mechanism of microbubble ascent in fractures cannot. Over a narrow range of fracture apertures, rapid vertical migration can occur at a flux low enough to preserve accumulations for geological lengths of time. Rapid ascent is also likely in fractures having wide apertures, but the rate of gas loss is too great to be sustained by modest accumulations for geological time. Continuous gas-phase migration initiates before gas-bubble migration in a fracture of fixed aperture, because the capillary pressure needed for a continuous gas phase to enter a fracture is less than that needed to form a bubble that could enter the same fracture.

Real fracture networks are much more complex than the simple parallel plate model used in this article, but the relative velocity of the studied mechanisms are not greatly affected by the complexity. Volumetric flux is affected by the complexity of real fracture networks and by the effects of gas expansion as it ascends. For example, realistic fracture networks probably have a capillary displacement pressure that may cause the pressure valve effect reported in the literature.

Although in this article I provide a theoretically justified mechanism for surface microseepage, the narrow aperture range over which this process can occur effectively calls into question the actual controls on distribution of geochemical anomalies: accumulations or fractures? Perhaps integration of fracture characterization studies and surface geochemical analysis will help overcome this ambiguity.

REFERENCES CITED

Allen, J. R. L., 1984, Sedimentary structures their character and physical basis, volume 1, New York, Elsevier, 593 p.

Araktingi, R., M. Benefield, Z. Bessenyei, K. Coats, and M. Tek, 1984, Leroy storage facility, Uinta County, Wyoming: a case history of attempted gas-migration control: Journal of Petroleum Technology, v. 34, p. 132–140.

Arp, G. W., 1992a, Effusive microseepage: a first approximation model for light hydrocarbon movement in the subsurface: Association of Petroleum Geochemical Explorationists Bulletin, v. 8, p. 1–17.

Arp, G. W., 1992b, An integrated interpretation for the origin of the Patrick Draw oil field sage anomaly: AAPG Bulletin, v. 76, p.301–306.

Brodkey, R. S., 1967, The phenomena of fluid motions: Reading, Massachusetts, Addison-Wesley Publishing, 737 p.

Brown, A. A., 1999, Predicting preservation and destruction of accumulations, *in* E. A. Beaumont and N. H. Foster, eds., Exploring for oil and gas traps: AAPG Treatise of Petroleum Geology Handbook of Petroleum Geology, p. 11-1–11-30.

Churchill, S. W., 1988, Viscous flows: the practical use of theory: Boston, Butterworths Publishers, 602 p.

England, W. A., A. S. Mackenzie, D. M. Mann, and T. M. Quigley, 1987, The movement and entrapment of petroleum fluids in the subsurface: Journal of the Geological Society, v. 144, p. 327–347.

Happel, J., and H. Brenner, 1965, Low Reynolds number hydrodynamics with special applications to particulate media: Englewood Cliffs, New Jersey, Prentice-Hall, 553 p.

Horwitz, L., 1969, Hydrocarbon geochemical prospecting after 20 years, *in* W. Heroy, ed., Unconventional methods in exploration for petroleum and natural gas: Dallas, Southern Methodist University Press, p. 205–218.

Huitt, J. L., 1956, Fluid flow in simulated fractures: American Institute of Chemical Engineers Journal, v. 2, no. 2, p. 259–264.

Jones, V. T., and S. G. Burtell, 1996, Hydrocarbon flux variations in natural and anthropogenic seeps, *in* D. Schumacher and M. Abrams, eds., Hydrocarbon migration and its near-surface expression: AAPG Memoir 66, p. 203–221.

Klusman, R. W., and M. E. Jakel, 1998, Natural microseepage of methane to the atmosphere from the Denver-Julesburg basin, Colorado: Journal of Geophysical Research, v. 103, no. D21, p. 28041–28045.

Klusman, R., and M. Saeed, 1996, Comparison of light hydrocarbon mechanisms, *in* D. Schumacher and M. Abrams, eds., Hydrocarbon migration and its near-surface expression: AAPG Memoir 66, p. 157–168.

Krooss, B. M., and D. Leythaeuser, 1996, Molecular diffusion of light hydrocarbons in sedimentary rocks and its role in migration and dissipation of natural gas: *in* D. Schumacher and M. A. Abrams, eds., Hydrocarbon migration and its near-surface expression: AAPG Memoir 66, p. 173–183.

Leythaeuser, D., R. G. Schaefer, and A. Yukler, 1982, Role of diffusion in primary migration of hydrocarbons: AAPG Bulletin, v. 66, p. 408–429.

Link, W. K., 1952, Significance of oil and gas seeps in world oil exploration: AAPG Bulletin, v. 36 no. 8, p. 1505–1540.

MacElvain, R., 1969, Mechanics of gaseous ascension through a sedimentary column, *in* W. Heroy, ed., Unconventional methods in exploration for petroleum and natural gas: Dallas, Southern Methodist University Press, p. 15–28.

Macgregor, D. S., 1996, Factors controlling the destruction or preservation of giant light oilfields: Petroleum Geoscience, v. 2, p. 197–217.

Price, L. C., 1986, A critical review and proposed working model of surface geochemical exploration, , M. J. Davidson, ed., Unconventional methods in exploration for petroleum and natural gas IV: Dallas, Southern Methodist University Press, p. 245–304.

Saunders, D. F., K. R. Burson, and C. K. Thompson, 1999, Model for hydrocarbon microseepage and related near-surface alterations: AAPG Bulletin, v 83, p. 170–184.

Schumacher, D., D. C. Hitzman, J. Tucker, and B. Rountree, 1997, Applying high-resolution surface geochemistry to assess reservoir compartmentalization and monitor hydrocarbon drainage, *in* R. J. Kruizenga and M. W. Downey, eds., Applications of emerging technologies: unconventional methods in exploration for petroleum and natural gas V proceedings: Dallas, Southern Methodist University Press, p. 309–322.

Tedesco, S. A., 1999, Anomaly shifts indicate rapid surface seep rates: Oil and Gas Journal, v. 97, no. 13 p. 69–72.

Tucker, J., and D. Hitzman, 1996, Long term and seasonal trends in the response of hydrocarbon-utilizing microbes to light hydrocarbon gases in shallow soils, *in* D. Schumacher and M. A. Abrams, eds., Hydrocarbon migration and its near-surface expression: AAPG Memoir 66, p. 353–357.

Yang, Y., and A. Aplin, 1998, Influence of lithology and compaction on the pore size distribution and modelled permeability of some mudstones from the Norwegian margin: Marine and Petroleum Geology, v. 15, p. 163–175.